

Cavitation Phenomena Inside an Autoclave Containing a Chemically Active Bubbly Medium

K. MITROPETROS¹, P. A. FOMIN¹, A. RUCKELSHAUSEN²,
H. HIERONYMUS¹

¹ Federal Institute for Materials Research and Testing (BAM), Unter den Eichen 87, D-12205 Berlin, Germany

² FH-Osnabrück, Albrechtstraße 30, D-49009 Osnabrück, Germany

In this work, cavitation phenomena inside an autoclave that contains a chemically active bubbly medium were investigated. Such media are required to conduct processes, such as liquid-phase hydrocarbon oxidation. The liquid was cyclohexane and contained explosive gas bubbles of cyclohexane and oxygen. Rarefaction waves were created inside the medium by the impact of a detonation wave on its surface. High speed optical (100,000 fps) and pressure (1 Mhz) measurements were applied.

The behavior of the pre-existing explosive bubbles as well as of the cavitation bubbles during the propagation of a pressure wave with positive and negative phase was optically recorded. This behavior was simulated by calculation. The calculated results correlate reasonably well with the experimental observations.

Additionally, the influence of the internal geometry of the liquid's vessel on the existence of cavitation phenomena is experimentally demonstrated. It was found that asymmetries in the cylindrical volume of the liquid, vertical to the propagation direction of a rarefaction wave, disturb or eliminate this wave.

Keywords: Bubble; Cyclohexane; Dynamics; Detonation; Shock wave; Rarefaction wave; Explosion; Shock induced

1. Introduction

If a liquid is subjected to a decreasing pressure at constant temperature, and the pressure falls below the saturated vapor pressure, then a process of rupturing takes place. This process is often called *cavitation*. Cavitation caused by a decrease of pres-

sure appears in fluid flow, such as with ship propellers, hydrofoils, pipes and pumps. It can also occur in sound fields in the underpressure cycle of the sound wave [1]. The cavitation bubbles origin from micro-inhomogeneities inside the liquid, which are often called *cavitation nuclei*.

There are two major kinds of cavitation nuclei. The microbubbles of free gas is the first one. They may be present in crevices within the solid boundary or within suspended particles or could simply be freely suspended within the liquid. Temporary, microscopic voids formed due to the thermal motions within the liquid is the second one.

Further kinds of cavitation nuclei exist. For example, nuclei can be formed by local energy deposit in the form of either heat, light or particles. These kinds of cavitation nuclei are expected to be of minor importance for the experiments that are reported in this paper.

Cavitation is accompanied by a number of effects. Cavitation bubbles tend to collapse exceedingly fast, emitting shock waves and even light (sonoluminescence). Perhaps the two most ubiquitous safety engineering problems caused by the collapse phase of cavitation bubbles are the material damage (erosion) that can be caused when the collapse takes place in the vicinity of a solid surface, and the fact that chemical reactions in the liquid can be induced.

For the case of cavitation erosion, it has long been recognized that the action of n bubbles is greater than n times the action of one. Nevertheless the single bubble behavior remains the basis of the destruction mechanism. Theoretical calculations for the collapse of cavitation bubbles have shown that pressures as high as 10^4 bar can be locally produced ([2], [3]). The damage potential of such pressures was experimentally demonstrated by several authors (e.g. in [4], [5]). These pressures, however, fall off very quickly within a few bubble radii [6].

If the collapse process of the bubble takes place within a reactive material, then the potential to start local reaction leading to partial decomposition or run to full detonation exists [7]. The stimulus for ignition is local high temperatures, i.e. the formation of the so called *hot spots*. These temperatures are created by three different ways during the bubble collapse [8]. The one is that the temperature rises inside the collapsing bubble due to compression. The second is that in case of asymmetric bubble collapse a shock-heated region is formed at the position where the liquid jet hits the surface of the bubble during its penetration. The third way demonstrates itself more intensively in viscous liquids. The friction between the gas phase of the bubbles and its high speed shrinking surface heats the surrounding liquid. The heating effect is enhanced in case of a liquid jet penetration during the bubble collapse, through the additional surface where friction takes place.

In this work cavitation phenomena inside an autoclave that contains a chemically active bubbly medium were investigated. Such media are required to conduct processes, such as liquid-phase hydrocarbon oxidation. An example is the oxidation of cyclohexane to cyclohexanone and cyclohexanol, which is used as raw material for the production of nylon.

One part of the motivation for these investigations was to observe the explosion behavior of the medium in the case that a pressure wave with periodic positive and negative phase propagates inside it. The other part of the motivation was to investigate the role of the vessel's geometry on the existence of cavitation phenomena inside it. This was possible by variation of the internal shape of the autoclave.

In order to better understand the observed cavitation behavior, a calculation of the bubble dynamics under the experimental conditions is presented. By comparison of these results with the optical observations, the negative part of the pressure signal in the experiments is estimated.

2. Experimental

2.1. Experimental setup

The autoclave consists of mainly three parts (see Fig. 1). In the bottom part (part I) the bubble generator is installed. Additionally, part I contains four adapters for pressure transducers and windows. The diameter of the openings hosting these adapters is 100 mm. The inner diameter of the bottom part can be either 200 mm or 100 mm. In the experiments reported in this work, only the diameter of 100 mm was used. The middle part (part II) and the upper part of the autoclave (part III) have an inner diameter of 100 mm, too. On the upper part the ignition source is installed. As ignition source an exploding wire was used. The total length of the autoclave is 1,070 mm. The bubble generator in the bottom of the autoclave consists of an orifice with two side openings of 0.35 mm diameter each. The outlet for the liquid is installed in the bottom part of the autoclave too.

The length of the acrylic glass window was either 40 mm, 144 mm, or 184 mm. Metallic sealing gaskets were used on the two longer windows on the right, as seen in Fig. 2. At 184 mm the windows filled almost completely the corresponding openings of the autoclave, so that the volume of the liquid inside had a cylindrical form.

In the case when two acrylic glass windows were used (i.e. the internal volume of the autoclave was cylindrical), the liquid phase amounted to 2 400 ml pure cyclohexane. The surface of the liquid was situated 350 mm from the bottom of the autoclave, reaching the level shown in Fig. 1, independent of the type of windows that were used.

The mole fraction of acetylene and oxygen in the explosive mixture above the liquid phase were 0.25 and 0.75 respectively. All experiments were performed at room temperature (20°C–25°C) and at initial pressure 1 bar.

The window type 1 offers an observation area of 10 cm in diameter. Due to the metallic sealing gaskets that are installed, the windows of type 2 and 3 offer an observation area of 9 cm in diameter.

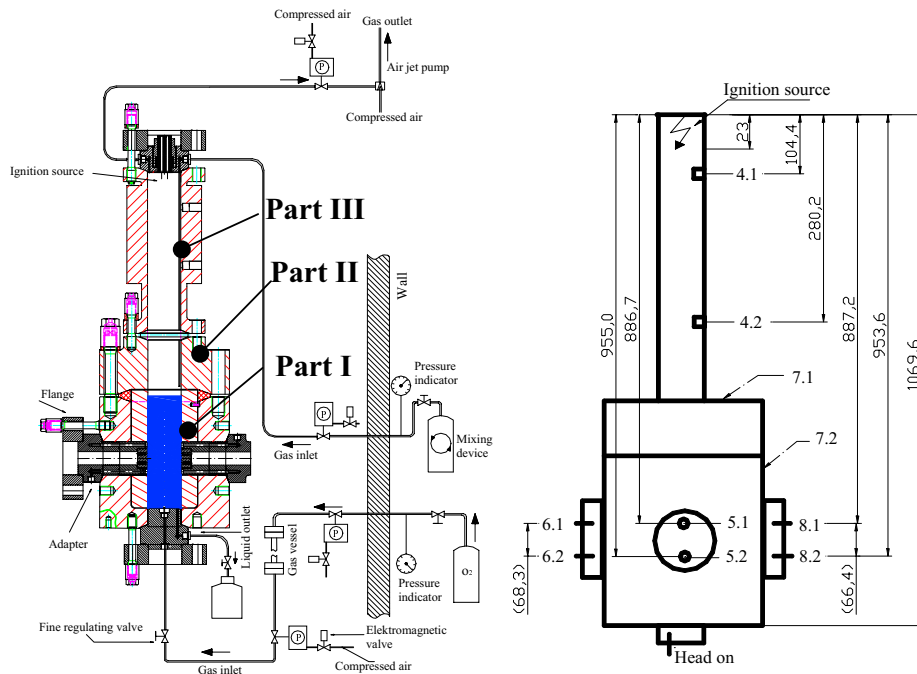


Fig. 1. Two schematics of the autoclave. On the right one the positions of the pressure sensors are annotated.



Fig. 2. Three different acrylic glass windows.

2.2. Experimental procedure

The experimental procedure was the following. First the appropriate volume of liquid is imported into the autoclave. Then an explosive acetylene-oxygen gas mixture

is fed in from the upper gas inlet. Bubbles are created by injecting gaseous oxygen into the liquid phase through the bubble generator on the bottom. The time interval until the bubbles reached the position of the observation window was enough for the vapors of the surrounding cyclohexane to saturate the oxygen bubbles [12]. Thus, the bubbles seen in the optical recordings of this work contained an explosive, nearly stoichiometric, gaseous mixture. A shock wave in the liquid is generated by a gas detonation of the explosive mixture above the liquid. The gas detonation is ignited by an exploding wire in the top flange of the autoclave.

2.3. Applied measurements techniques

Pressure and optical measurements were performed during each experiment. For the pressure measurements, piezoelectric pressure transducers (Kistler 601H) in combination with a multi-channel transient recorder operating at a sample rate of 1 MHz were used. The produced signal from the pressure transducers was then passed through an electronic amplifier of the type Kistler 5001 SN. The signal was intensified there, so that it could be recognized by the transient recorder. The transient recorder used in this work was the model TRA 800 from the company *W + W Instrumente AG Basel*.

The detonation pressure in the gas phase was measured from the pressure sensors at the positions indicated by 4.1 and 4.2 in Fig. 1. The pressure signals inside the liquid phase at the level of the windows, which are presented in this work, were recorded at the position 8.1 and at the bottom of the autoclave (Fig. 1).

The measured pressure signals were smoothed with a running average of 20 points (i.e. 20 μ s). The smoothing was necessary for reducing the influence of the natural oscillations of the pressure transducers. Averaging over 20 points corresponds to exactly 3 oscillation periods of the transducers.

The interaction of the bubbly liquid with the shock wave was observed with the help of a prototype digital highspeed framing camera of the company Shimadzu (model ISIS V2). It offers a maximum framing rate of 1,000,000 fps at a resolution of 312 x 260 pixels. The spatial resolution of the optical recordings presented in this work was about 0.35 mm/pixel. The exposure time of each frame is the interval time between the recording of two sequential frames. The camera offers a total of 104 digital frames. During the experiments, diffused light was used as external light source.

3. Results and Discussion

3.1 Cavitation phenomena inside a bubbly medium

The structure of the pressure signals inside the liquid medium is an important information that is connected with the existence of cavitation phenomena. In order to understand this structure, it is necessary to take into account that the result of the reflection of a pressure wave at the border between two different media depends on the relation of the acoustical impedance of these media (see [9] and [10]).

In Fig. 3 a schematic that shows the behavior of a shock wave inside the liquid phase of the autoclave, generated by the impact of a planar detonation wave on the surface of the liquid, is shown. After the impact of the detonation wave on the surface of the liquid, a reflected shock wave is created in the gas and also a shock wave inside the liquid, which propagates towards the bottom of the autoclave. It is then reflected as shock wave at this position, returning back to the surface of the liquid. At the surface it is reflected as a rarefaction wave and returns to the bottom again, where it is reflected as a rarefaction wave once more. The next reflection at the surface of the liquid creates a new shock wave. Each time a pressure wave (shock or rarefaction wave), propagating inside the liquid medium, is reflected at the surface of the liquid, a corresponding pressure wave is refracted into the gaseous medium (see Fig. 3).

Given that the pressure waves propagate with the sound velocity inside the liquid, i.e. 1 280 m/s [11], these reflections should create a periodic change between shock wave (positive phase) and rarefaction wave (negative or zero phase) inside the liquid until they fade out. And in deed this effect was observed in the experiments, independent of the existence of gas bubbles inside the liquid. This is because although an adequate number of bubbles inside the liquid can change the structure of the pressure signal, as illustrated in Fig. 4, the existence of the subsequent positive – negative phases can not be prohibited.

At this point it is necessary as background information to know that a pressure wave propagating in a liquid with bubbles has an oscillatory structure. This is a known characteristic feature of bubbly liquids (see e.g. [19] - [21], [22]). This feature is illustrated in Fig. 4 for three different cases: (i) the evolution of a pressure step into its final steady form is sketched; (ii) indicates the development of the shock wave into a train of solitons as a result of the action of a negative wave packet; and (iii) shows the evolution of a negative wave packet. Since the speed of the single peaks increases with amplitude, they move up the slope of the rarefaction wave.

There are some further effects that during the experiments influenced the structure of the pressure signal inside the liquid. The most dominant of these additional effects are three. First of all, the pressure of the detonation wave that impacted the surface of the liquid at the beginning of the process, had a spatial gradient, i.e. it was not a step wave. Secondly in the gas phase of the autoclave, due to shock wave reflections and due to the periodic addition of refracted waves created at the liquid's surface, the pressure was strongly time dependent. Finally the structure of the measured pressure signals was influenced by the damping effect during the propagation of all the pressure waves inside the system.

A typical example of the experimentally measured pressure behavior in a cylindrical autoclave is presented in Fig. 5. In Fig. 6 a schematic of the autoclave showing the position of the liquid's surface and the positions of the pressure measurements shown in Fig. 5 is presented.

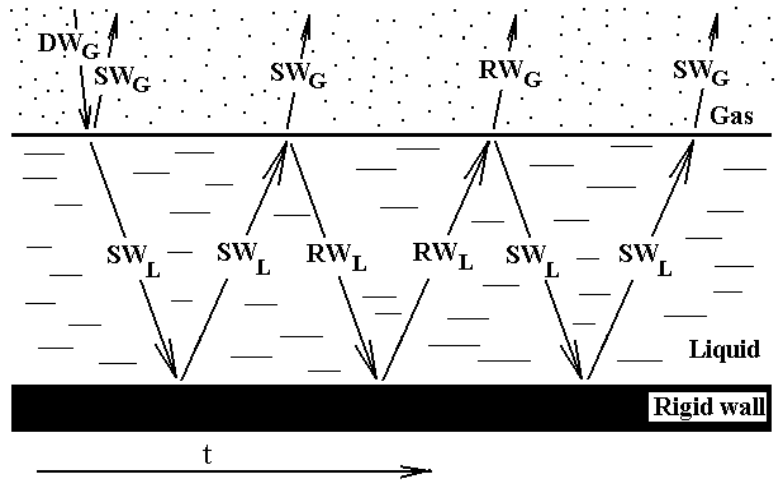


Fig. 3. The behavior of a shock wave inside the liquid phase of the autoclave, generated by the impact of a planar detonation wave on the surface of the liquid.
 DW_G : detonation wave with its front parallel to the liquid's surface; SW_G : shock wave inside the gas phase; RW_G : rarefaction wave inside the gas phase; SW_L : shock wave inside the liquid phase; RW_L : rarefaction wave inside the liquid phase.

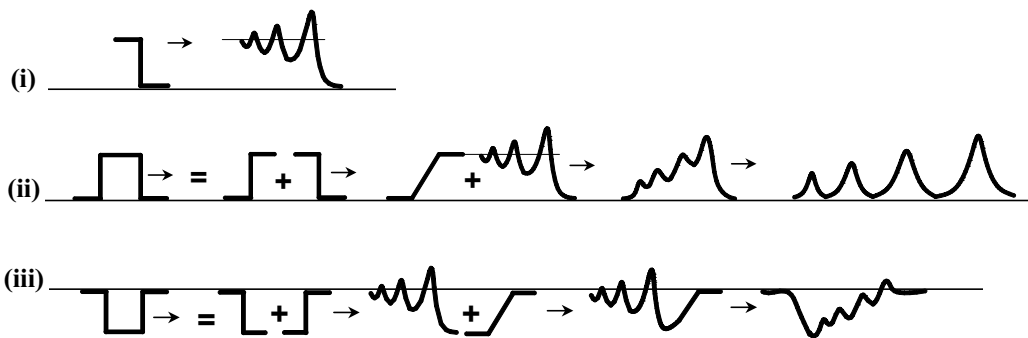


Fig. 4. Construction of wave shapes in a bubbly medium (inert bubbles).
 (i) Steady positive step wave (shock wave); (ii) The positive wave packet finally develops into a train of (steady) solitons; (iii) Negative wave packet. Solitons finally creep up the slope of the rarefaction wave. The wave shapes correspond to the suggestion in [22].

In Fig. 5 the following parts of the signal can be recognized. The shock wave peak pressure that was created from the detonation impact on the surface propagating towards the bottom of the autoclave (pos. 1); the reflection on the bottom propagating towards the surface (pos. 2) first passing in front of the observation window (pos. 3). After the shock wave impact at the surface, it is reflected as rarefaction wave propagating towards the bottom. This rarefaction wave is recorded first by the pressure sensor at the level of the windows (pos. 4) and then by the sensor at the bottom of the auto-

clave (pos. 5). The structure is distorted after a few reflections as the pressure wave in the liquid becomes weaker and the influence of the pressure behavior in the gas phase, more important.

In Fig. 7 the optical recordings that correspond to the experiment shown in Fig. 5 are presented. The initial diameter of the bubbles seen in this figure was between 2 mm and 4 mm. The passage of the shock wave did not ignite all the bubbles. In Fig. 7 three of the observed bubble explosions can be seen (at 30 μs ; 80 μs and at 90 μs). The fact that some of the bubbles did not ignite, may be explained by the shock induced jet penetration inside them [12]. This jet enriches the bubble in cyclohexane vapors and possibly allows its gas phase to exceed very fast the explosion limits.

The rarefaction wave entered the observation window during the frame recorded at 620 μs . As the rarefaction propagates through the liquid a zone of cavitation bubbles appears. The cavitation bubbles appear almost homogeneously in all the volume and reach a maximum radius of about 2 mm. The cavitation starts to disappear after about 300 μs (Fig. 7, 920 μs).

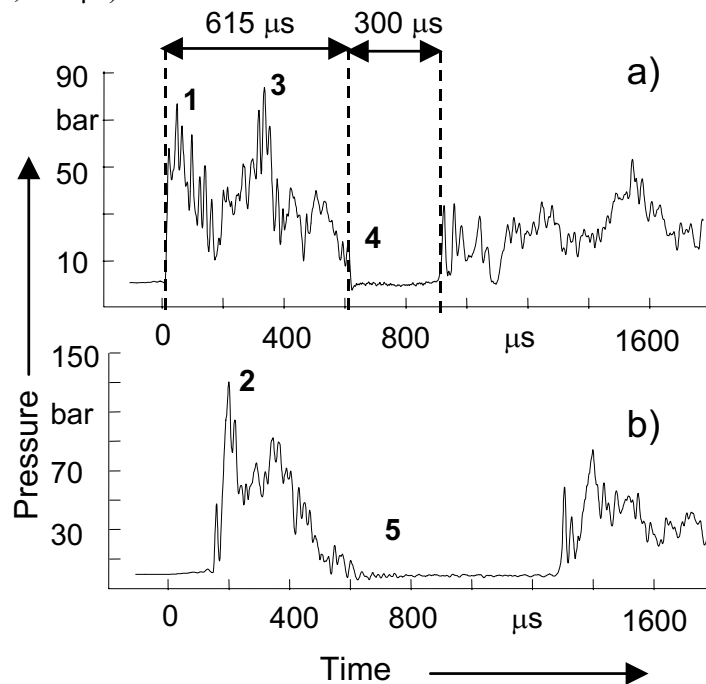


Fig. 5. Pressure signals recorded during an experiment where the bubbly liquid had cylindrical volume.

The pressure curves (a) and (b) were measured at the positions (a) and (b) in Fig. 6 respectively. The numbers on both signals indicate the sequence of the pressure wave passage from the two pressure sensors. The geometry of the autoclave was cylindrical (windows length: 184 mm) and the height of the liquid 35 cm. During the duration of such relatively strong rarefaction waves, cavitation bubbles can be produced inside the bubbly liquid. Such a behavior can be seen in Fig. 7.

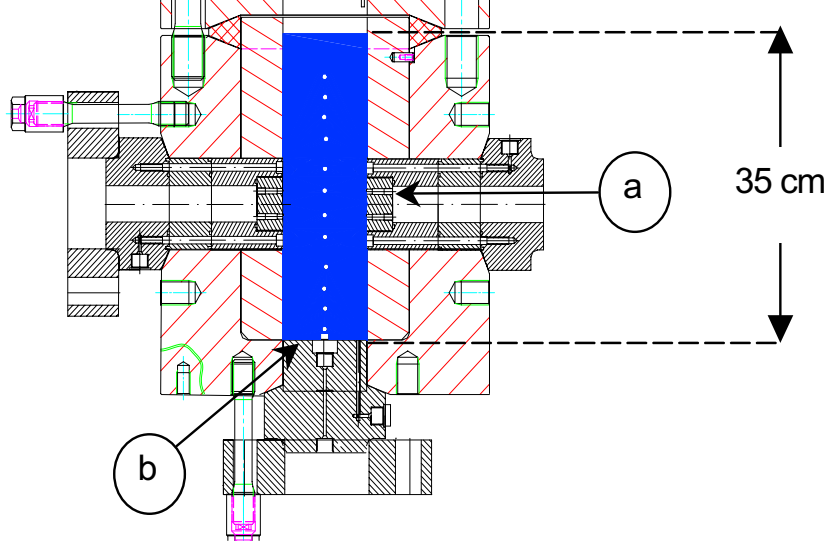


Fig. 6. Cut out of the autoclave.

This schematic shows the position of the pressure sensors for the pressure measurements during the experiment presented in Fig. 5.

The bubble dynamics was calculated. For the calculation the pressure signal in Fig. 5a was simulated and the bubbles were assumed to be spherical. The bubble dynamics is described by the Rayleigh-type equation [13]:

$$\beta \frac{d^2 \beta}{dt^2} + \frac{3}{2} \cdot \frac{1}{\beta} \cdot \left(\frac{d\beta}{dt} \right)^2 = \left(\bar{P} - \frac{P_L}{P_0} \right) \frac{P_0}{\rho_L R_0^2}, \quad (1)$$

$$\bar{P} = \frac{1}{P_0} \cdot \left(P - \frac{2\sigma}{R} \right) - \frac{4}{\beta} \cdot \frac{\rho_L \nu_L}{P_0} \cdot \frac{d\beta}{dt} - 3 \frac{\rho_0}{\beta^3 P_0} \cdot \frac{R_0}{C_L} \left(1 + \frac{P - P_L}{B - P_L} \right)^{-\frac{1}{n}} \frac{dP}{d\rho} \cdot \frac{d\beta}{dt}.$$

Here R is the bubble radius, $\beta = R/R_0$ is the dimensionless radius of the bubble, ρ and ρ_L are the gas and liquid density, P is the pressure of the gas, ν_L , C_L and P_L are the cinematic viscosity, velocity of sound and pressure of the liquid, B and n are the constants of Tait equation of state of the liquid, t is the time. Index “0” corresponds to the initial stage, the time moment $t = 0$ corresponds to the start of bubble dynamics.

Note, that compared with the classical Rayleigh equation for bubble dynamics, equation (1) takes into account the compressibility of the liquid and the energy losses owing to the viscosity and the acoustic radiation from the bubble.

The gas is assumed to be ideal:

$$\frac{P}{\rho} = \frac{\mathfrak{R}T}{\mu}. \quad (2)$$

Here T and μ are the temperature and molar mass of the gas, \mathcal{R} is the universal gas constant.

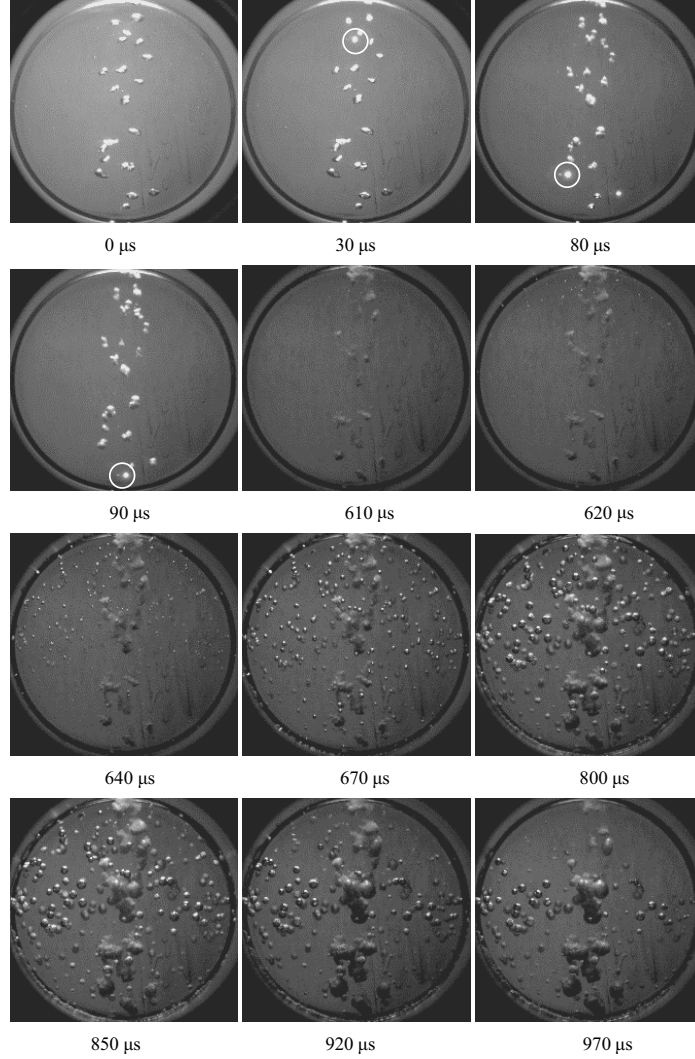


Fig. 7. Gas bubbles in cyclohexane under shock wave and subsequent rarefaction wave impact.

The white circles indicate exploding bubbles. The observation area had a diameter of 90 mm. Windows of type 3 were used (windows length: 184 mm, see Fig. 2). Time zero corresponds to the moment the shock wave entered the observation window. The pressure in the liquid is the curve (a) in Fig. 5.

The bubble compression and expansion are assumed to be adiabatic. The adiabatic curve and the adiabatic index γ of the gas are described according to [14]:

$$\frac{dT}{d\rho} = \frac{\Re T / \rho \mu}{U_T}, \quad \gamma = \frac{d \ln P}{d \ln \rho} = 1 + \frac{\rho}{T} \cdot \frac{dT}{d\rho}. \quad (3)$$

Here U_T is the temperature derivative of the specific internal energy U of the gas. This energy is calculated by the formula:

$$U(T) = \alpha_{O_2} U_{O_2}(T) + \alpha_{C_6H_{12}} U_{C_6H_{12}}(T). \quad (4)$$

Here α_{O_2} , $\alpha_{C_6H_{12}}$ and U_{O_2} and $U_{C_6H_{12}}$ are the mass fractions and the specific internal energies of oxygen and cyclohexane respectively. The values U_{O_2} and $U_{C_6H_{12}}$ can be found in ([15] - [17]). Derivative U_T can be obtained from formula (4) and corresponding data of ([15] - [17]). Note, that formula (3) allows us to take into account, that adiabatic index of the gas depends on the temperature.

The constants $C_L = 1284$ m/s, $\rho_L = 7.8 \cdot 10^3$ kg/m³, $v_L = 1.06 \cdot 10^{-4}$ m²/s can be found in [18]. The follow exponent of the Tait equation of state of liquid cyclohexane is used: $n = 7$. Thus, $B = \rho_L C_L^2 / n = 1837$ bar.

The calculation has been performed for the following initial conditions: pressure of 1 bar and temperature of 298 K. The initial quantity of cyclohexane inside the bubble corresponds to the vapor pressure of the liquid at the initial conditions. As initial diameter of the cavitation nuclei 0.2 mm, and 0.4 mm was chosen. These sizes correspond to practically invisible bubbles for the recording shown in Fig. 7. For the bubbles that were created before the detonation impact on the liquid, the initial bubble diameters of 2 mm; 3 mm and 4 mm where chosen, as typical sizes for the experimental conditions.

Since the installed pressure sensors in the autoclave can not measure negative pressures, there is no adequate experimental information about its amplitude and its duration. Because of this reason the negative part of the signal has to be assumed.

In the ideal situation when the liquid would not contain any gas bubbles and the pressure wave propagating inside it would be a step wave; the amplitude of the negative part of the pressure signal should correspond to the characteristic amplitude of the positive part before it [13]. In the performed experiments the amplitude of the negative signal is expected to be less than in the just described ideal situation. This is so, because in the experiments the pressure wave has a complicated structure (as seen in Fig. 5a) and because of the fact that the existence of the bubbles in the system influence the pressure behavior inside it. The total duration of the negative part of the signal should correlate with the experimentally measured zero level of the pressure. Taking into account this information, the pressure profile shown in Fig. 8 was used for the calculation of the bubble dynamics. This pressure field simulates the pressure signal, presented in Fig. 5a Fig. 5a. The duration of the negative part of the pressure in Fig. 8 equals to the duration of the zero signal of Fig. 5a. It is assumed, that the amplitude of the negative pressure reached linearly the value of -5 bar (see Fig. 8).

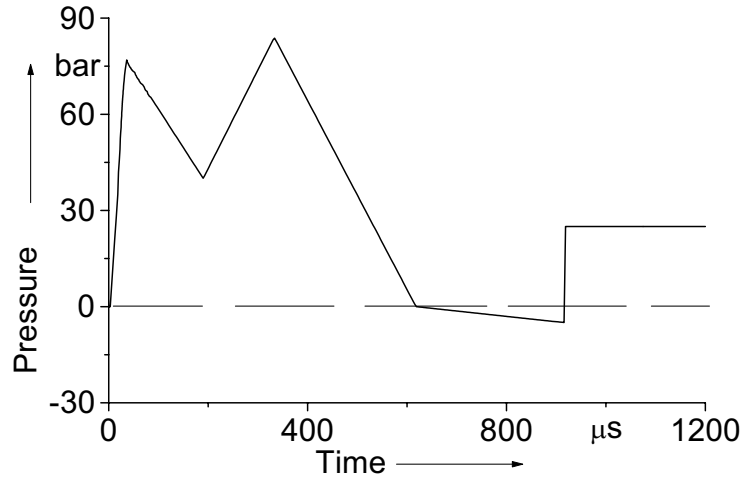


Fig. 8. The profile of the pressure, which was used for the calculations. The dashed line indicates the zero level of the pressure. Time zero corresponds to the same point in Fig. 5a.

The calculated diameter of the pre existing gas bubbles and of the cavitation bubbles is presented in Fig. 9 and Fig. 10 respectively. During the cavitation conditions the diameter of the pre-existing and cavitation bubbles significantly increases and then violently collapses (Fig. 9 and Fig. 10). As an example, in Fig. 9 it can be seen that a gas bubble with initial diameter of 3 mm is reduced to less than 1 mm because of the shock wave impact and expanded to up to 10.8 mm, at 946 μs , as a result of the rarefaction wave passage. According to the calculation the size of the pre-existing bubbles due to violent collapse reaches the minimum value at 1050 μs . An expanding nuclei

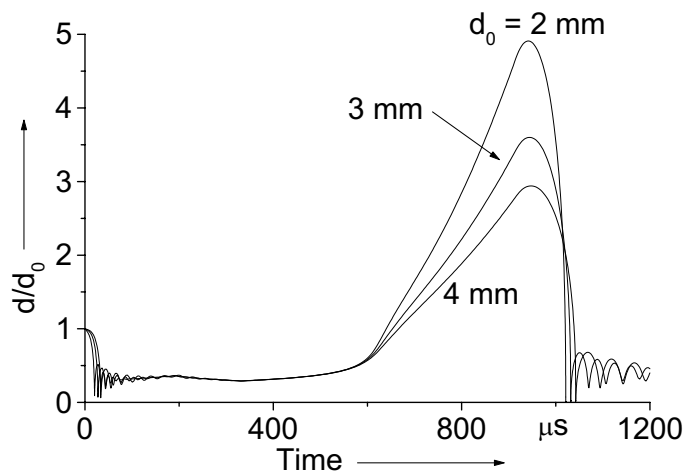


Fig. 9. Calculated radius of gas bubbles in the pressure field, presented in Fig. 8.

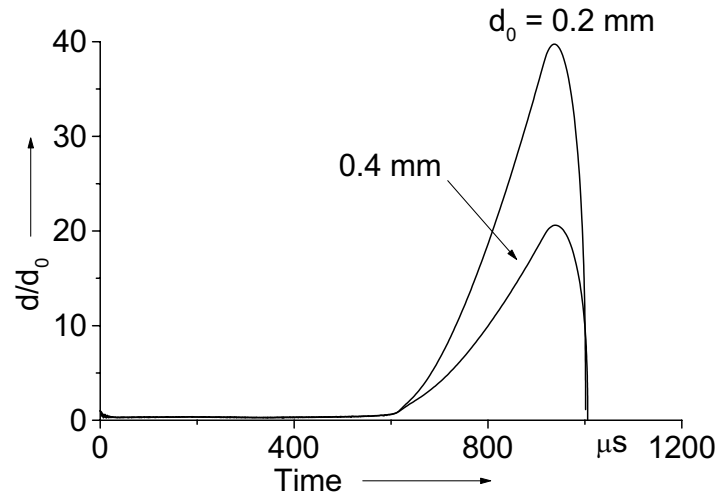


Fig. 10. Calculated radius of cavitation bubbles in the pressure field, presented in Fig. 8.

becomes visible when its size corresponds to at least a few (2–3) pixels. Taking into account the spatial sensitivity of the frames presented in Fig. 7, one can estimate with the help of Fig. 10 the time from which the cavitation bubbles should become visible. This time is 630 μs to 680 μs for a nuclei with initial diameter between 0.2 mm and 0.4 mm. These nuclei reach their maximum size of about 8 mm at 940 μs and become invisible again after 1000 μs . All the calculated results presented above correlate reasonably well with the experimental observations in Fig. 7.

As nuclei, microbubbles of 0.2 mm and 0.4 mm in initial diameter were assumed.

Note that a different assumption about the maximum amplitude of rarefaction wave would create a quantitative deviation from the above calculated values, but it would not influence the qualitative results. For example, if the amplitude of the rarefaction wave in the pressure profile shown in Fig. 8 would reach the value of -10 bar instead of -5 bar, then the calculation of the bubble dynamics would give the following results. The maximum size of a pre-existing bubble 3 mm in initial diameter would be 14.1 mm, at 966 μs . A nuclei 0.2 mm in initial diameter, starts to become visible at a time between 648 μs to 665 μs (instead of 654 μs to 678 μs for -5 bar as maximum amplitude of the rarefaction wave). It then reaches a maximum size of about 11.7 mm at 958 μs and becomes invisible again after 1050 μs .

3.2. Influence of the geometry of the autoclave

The pressure structure in the liquid was discussed above only for the case in which the internal volume of the autoclave that contained the liquid was cylindrical, i.e. the windows that were used were of the type 3 (length: 184 mm), as denoted in Fig. 2.

In Fig. 11 the pressure signals measured in an experiment in which windows of type 1 (40 mm length) were used, is presented. The system consisted of liquid cyclohexane containing oxygen bubbles. In this figure it is not possible to clearly recognize parts of the signal that would correspond to the parts described for the pressure signals in Fig. 5. The pressure signals in Fig. 11 appear to be without a clear structure pattern, i.e. subsequent positive and negative (or zero) pressure phases were not registered. After the passage of the shock wave, the pressure inside the liquid tends to oscillate around -and finally reach- a value, which is the pressure of the gas phase after the detonation. In the experiments this value was about 10 bar to 30 bar at about 1 ms after the shock wave passage.

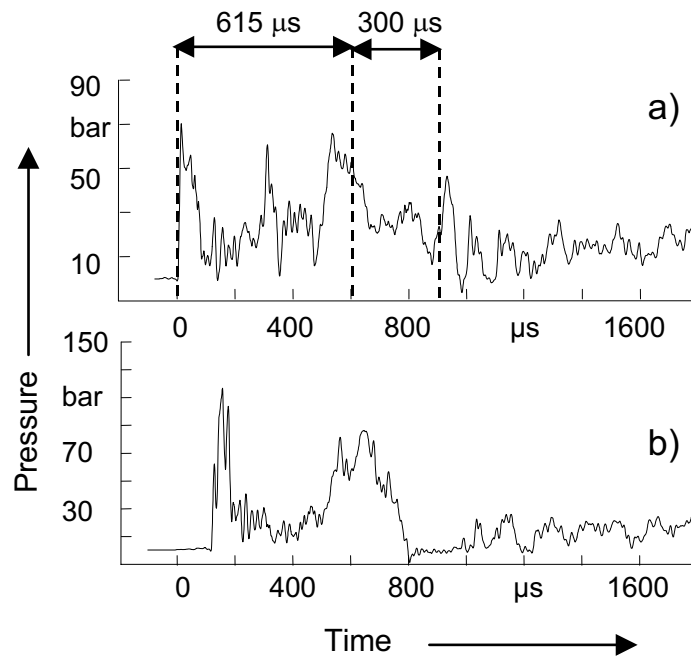


Fig. 11. Pressure signals recorded during an experiment during which the liquid had no cylindrical volume.

The optically recorded behavior of the system is presented in Fig. 12. In this figure the white circles indicate bubble explosions after the passage of the shock wave. In contrast to what was observed in Fig. 7, no cavitation bubbles were recorded in this experiment. This observation is in agreement with the absence of long negative (or zero) pressure levels that was observed in the pressure signals of the experiments, as described above.

Similar observations were made in all the experiments where the internal volume of the autoclave containing the liquid was not cylindrical. It is expected that the difference in the behavior is caused by the change of the geometry. This creates a more

complicated pressure signal in the liquid due to more complex pressure wave reflections in the volume.

The pressure curves a) and b) were measured at the positions a) and b) in Fig. 6 respectively. The geometry of the autoclave was not cylindrical (windows length: 40 mm) and the height of the liquid was 35 cm. For comparison reasons with Fig. 5, the times 615 μs and 300 μs later have been pointed.

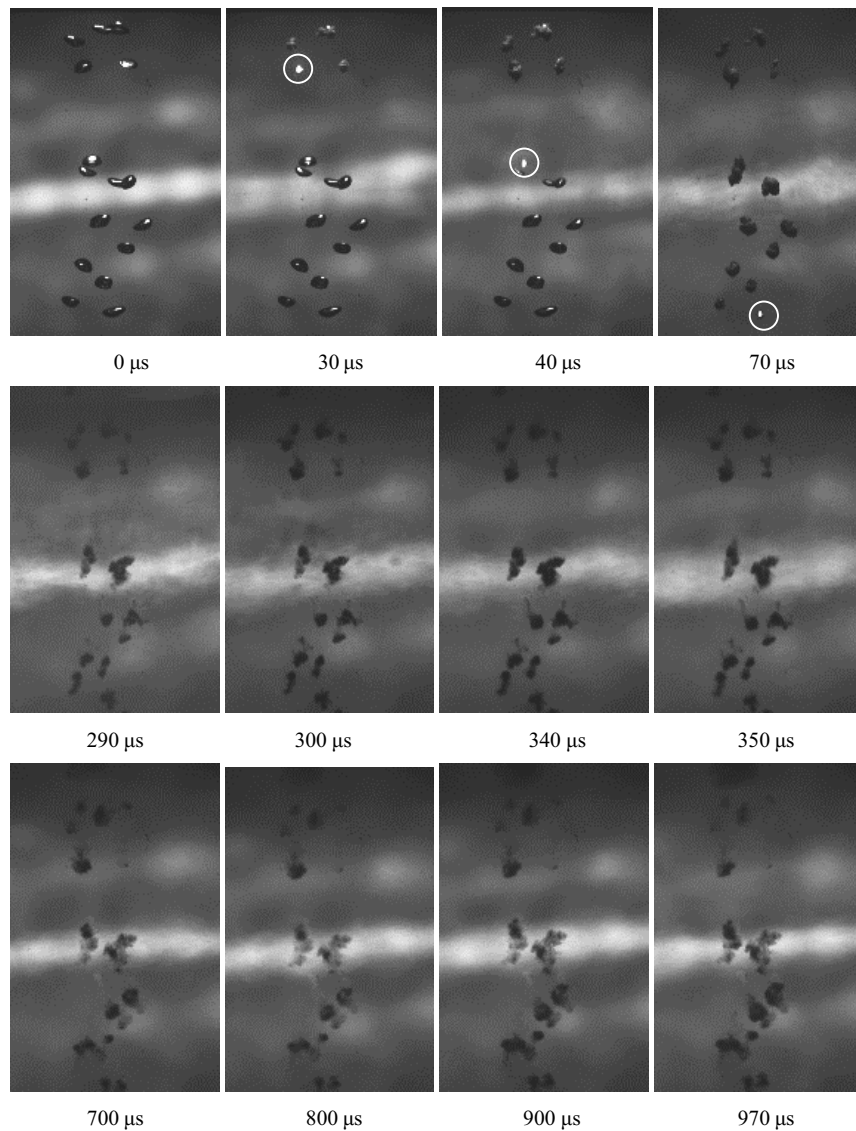


Fig. 12. Oxygen bubbles in cyclohexane under shock wave without subsequent rarefaction wave impact.

The white circles indicate exploding bubbles. The bubbles had an initial diameter between 3 mm and 3.5 mm. Windows of type 1 were used (windows length: 40 mm see Fig. 2). The framing rate was 100 000 fps. Time zero corresponds to the moment the shock wave entered the observation window. The pressure in the liquid is presented by the curve (a) in Fig. 11.

4. Conclusions

Rarefaction waves were created inside a bubbly liquid. The form of the liquid's vessel is decisive for the existence of these rarefaction waves through its entire volume. Asymmetries in the volume, vertical to the propagation direction of the rarefaction wave, disturb or destroy the latter. Control of the properties of a rarefaction wave by adjusting the geometry, is a direction connected with the safety in many applications and need to be further investigated.

During cavitation conditions the diameter of already existing gas bubbles is significantly altered. As a result their inner temperature and pressure changes. This makes a bubble explosion impossible during cavitation, even if these bubbles contain an explosive mixture inside them. But more investigations are necessary to prove if this behavior could allow the formation of explosive bubbles and their subsequent ignition during the collapse phase, inside chemically active bubbly liquids.

The structure of the pressure inside the liquid during and after the pressure wave's passage was also discussed. Its oscillatory structure is in agreement with the corresponding observations described in the literature. Apart from the oscillations, the positive to zero pressure level changes, i.e. the shock wave to rarefaction wave changes, and their duration are explained according to the sources of shock wave reflections inside the autoclave.

The experimentally observed behavior of the pre existing bubbles, as well as of the cavitation bubbles was theoretically described. The results of the calculation correspond to the experimental observations. According to the calculated results the negative part of the pressure signal in the experiments had an amplitude of about -5 bar.

Acknowledgements

This research project is financially supported by the Deutsche Forschungsgemeinschaft (DFG).

References

- [1] BRENNEN C.E.: Cavitation and bubble dynamics, Oxford University Press 1995.
- [2] PLESSET M.S., PROSPERETTI A.: Bubble dynamics and cavitation. *Ann. Rev. Fluid Mech.*, 9, 1971, p. 145.
- [3] MØRCH K.A.: Dynamics of cavitation bubbles and cavitation liquids, in *Erosion*. (Ed. C. M. Preece), Academic 1979, pp. 309-353.

-
- [4] BRUNTON J. H.: Erosion by liquid shock. Proc. 2nd Intl Conf. On Rain Erosion (ed. A. A. Fyall & R. B. King), Royal Aircraft Establishment, UK, 1967, p. 291.
- [5] TOMITA Y., SHIMA A.: mechanisms of impulsive pressure generation and damage pit formation by bubble collapse. J. Fluid Mech. 169, 535-564.
- [6] HICKLING R., PLESSET M.S.: Collapse and rebound of a spherical bubble in water. Phys. Fluids, 7, 1964, pp. 7-14.
- [7] BOURNE N.K., FIELD J.E.: Bubble collapse and initiation of explosion. Proc. R. Soc. Lond. A 435, 1991, pp. 423-435.
- [8] BOURNE N.K.: On the collapse of cavities, Shock waves, Vol. 11, No. 6, 2002, pp. 447-455.
- [9] Physics of Shock Waves and High – Temperature Hydrodynamics Phenomena I. Ya.B.Zel'dovich and Yu.P.Raizer, Editors: Wallace D. Hayes and Ronald F. Probstein, Academic Press, New York – London 1966.
- [10] LANDAU L.D., LIFSHITZ E.M.: Fluid Mechanics (Landau and Lifshitz Course of Theoretical Physics, Vol. 6), Butterworth-Heinemann, 2nd edition, 1995.
- [11] CRC Handbook of Chemistry and Physics, 81th edition, CRC Press 2000.
- [12] MITROPETROS K., HIERONYMUS H., STEINBACH J., PLEWINSKY B.: Explosions of oxygen bubbles in cyclohexane, Chemical Engineering Journal, Vol. 97, Issues 2-3, 2004, pp. 151-160.
- [13] KEDRINSKII V.K.: Hydrodynamics of Explosion (Experiment and Models), Siberian Division of the Russian Academy of Sciences, Novosibirsk 2000 (in Russian).
- [14] FOMIN P.A., TROTSYUK A.V.: An approximate calculation of the isentrope of a gas in chemical equilibrium. Combustion, Explosion and Shock Waves, , Vol. 31, N 4, 1995, pp. 455-457.
- [15] VUKALOVICH M.P., KIRILLIN V.A., REMIZOV S.A., SILETSKY V.S., Timofeev V.N.: Thermodynamical properties of gases (*Termodinamicheskie svoistva gazov*), Mashgiz Publ., Moscow, 1953 (in Russian).
- [16] VARGAFTIC N.B.: Handbook of thermo-physical properties of gas and liquids (*Spravochnik po teplofizicheskim svoistvam gazov i zidkostey*), Fizmatgiz, Moscow, 1963 (in Russian).
- [17] GLUSHKO V.P.: Thermodynamic Parameters of Individual Substances (*Termodinamicheskie svoistva individual'nih veshstv*), Vol. 2, Izdatel'stvo Akademii Nauk SSSR, Moscow 1962 (in Russian).
- [18] KIKOIN I.K. (ed.). Tables of Physical Quantities, Atomizdat, Moscow 1976 (in Russian).
- [19] NOORDZIJ L., VAN WIJNGAARDEN L.: Relaxation effects, caused by relative motion, on shock waves in gas-bubble/liquid mixtures. J. Fluid Mech. 66, 1974, pp. 115-144.
- [20] BORISOV A.A., GELFAND B.E.: TIMOFEEV E.I.: Shock waves in liquid containing gas bubbles. Int. J. Multiphase Flow 9, 1983, pp. 531-543.
- [21] Wave Propagation in Gas-Liquid Media. V.E.Nakroyakov, B.G.Pokusaev, I.R.Schreiber, CRC Press 2000.
- [22] BEYLICH A.E., GÜLHAN A.: On the structure of nonlinear waves in liquids with gas bubbles. Phys. Fluids A 2, 1990, p. 1412.